

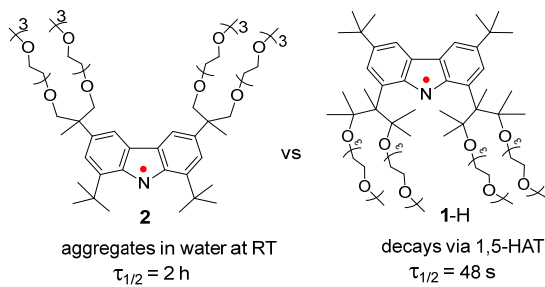
PEGylated, Water Soluble, Stable Aminyl Radical

Ying Wang, Suchada Rajca, Andrzej Rajca*

Department of Chemistry, University of Nebraska, Lincoln, Nebraska 68588-0304

E-mail address: arajca1@unl.edu

Table of Contents Graphics



Abstract: We report the synthesis and kinetic study of PEGylated, water soluble aminyl radical **2**. The radical possesses four mPEG-3 groups replacing four methyl groups in the *tert*-butyl groups at the 3- and 6-positions of 1,3,6,8-Tetra-*tert*-butyl carbazyl (TTBC). This structure is designed to mitigate the rapid decomposition of the radical via intramolecular 1,5-hydrogen atom transfer (1,5-HAT) that was observed in its constitutional isomer **1-H** with four mPEG-3 groups in the vicinity of the nitrogen-centered radical (1- and 8-positions of TTBC). In dry, degassed acetone at 295 K, the radical **2** has a half-life, $\tau_{1/2} = 49 \text{ h}$ ($\Delta H^\ddagger = 17.9 \pm 0.8 \text{ kcal mol}^{-1}$), which is 3 orders of magnitude longer than that for **1-H**, which decays via 1,5-HAT ($\tau_{1/2} = 48 \text{ s}$, $\Delta H^\ddagger = 10.0 \pm 0.3 \text{ kcal mol}^{-1}$). Aminyl radical **2** aggregates at ambient conditions in water and has a half-life, $\tau_{1/2} = 2 \text{ h}$.

Introduction

Stable, water soluble organic radicals have received great attention due to their potential applications in biology, biophysics, and biomedicine.¹⁻⁷ Most recent developments in the design and synthesis of these radicals have been tailored to their applications as spin labels and agents for DNP.^{8,9} Meanwhile, our interest focuses on development of organic radical contrast agent (ORCA) for magnetic resonance imaging, in which we recently demonstrated the efficacy of mPEGylated polynitroxide scaffolds.^{10,11}

Nitrogen-centered (aminyl) radicals have been mostly studied as reactive, short-lived intermediates. 1,3,6,8-Tetra-*tert*-butyl carbazyl (TTBC) is one of very few aminyl radicals that are stable at ambient conditions and can be isolated as solid (Figure 1),^{12,13} a highly attractive feature as building block for organic magnetic materials.¹⁴⁻²⁰ However, TTBC has received little attention since it was reported by Neugebauer and Fischer in 1971.^{12,19} We have considered derivatives of TTBC as potential molecular design framework to obtain stable, water soluble radicals for ORGA. Sterically shielded radicals with unpaired electrons centered at less electronegative atoms, such as nitrogen compared to oxygen, should possess more resistance to reduction *in vivo*. Because the less electronegative nitrogen is a better electron donor than oxygen, the hydrogen bonds to nitrogen, N---H-O, are among the strongest hydrogen bonds, typically stronger than O---H-O bonds.²¹ Thus, the aminyl-water hydrogen bond should be stronger (and shorter) than the analogous hydrogen bond in nitroxides. Due to the steep $1/r^6$ dependence for spin-spin interactions, it is likely that even slight shortening of the N---H vs. O---H distance could significantly increase ^1H water relaxivity,^{10a,22} based on the assumption that the rate of water exchange with aminyl radical is sufficiently fast.^{10a,22,23}

We recently prepared the methoxy polyethylene glycol (mPEG) substituted aminyl radical (1-H),²⁴ a mPEGylated derivative of TTBC. Our hypothesis was that hydrophilic derivatives of the hydrophobic *tert*-butyl groups in TTBC would provide solubility in water while maintaining adequate stability. However, we found that 1-H decays rapidly at room temperature (half-life, $\tau_{1/2} < 1$ min) via intramolecular 1,5-hydrogen atom transfer (1,5-HAT), which is facilitated by lowered bond dissociation energies in the

OC-H fragments of the mPEG-3 chains. The D₈-isotopomer, **1-D**, had a much longer half-life, $\tau_{1/2} > 1$ h, with extremely large kinetic isotope effect $k_H/k_D \approx 150$ at 298 K in acetone.²⁴

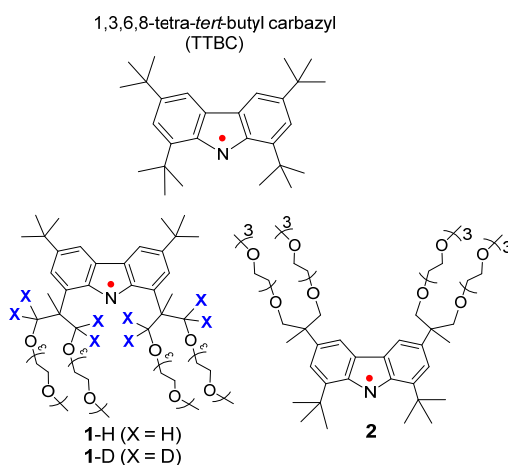


Figure 1. TTBC and its PEGylated derivatives: aminyl radicals **1-H**, **1-D**, and **2**.

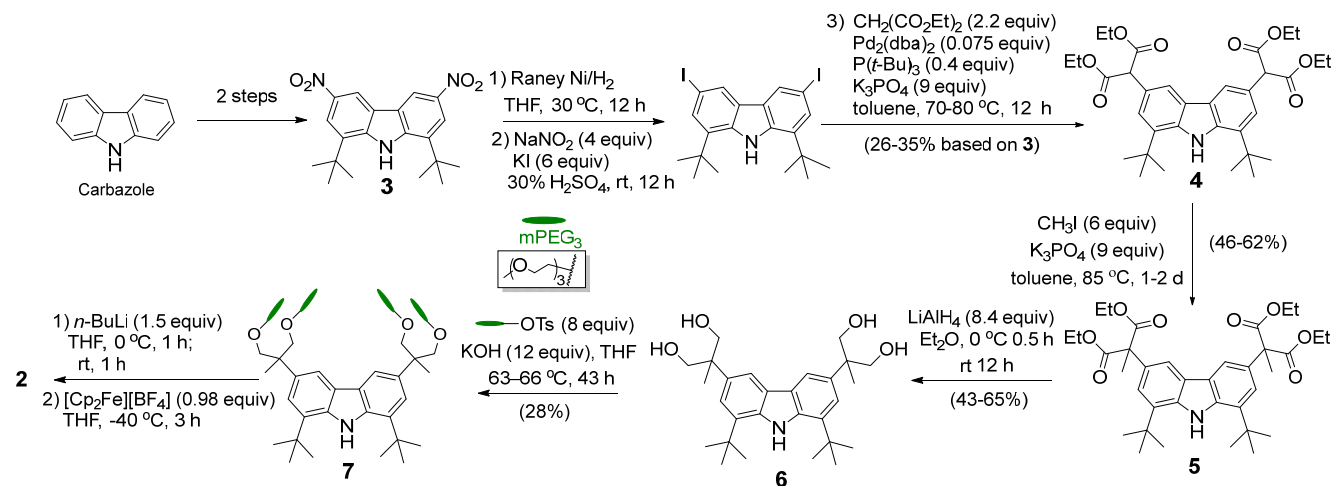
Here we report the synthesis and characterization of another mPEGylated derivative of TTBC, radical **2**, in which the mPEG-3 chains are not within close proximity of the aminyl radical moiety to mitigate the facile 1,5-HAT, which was observed in **1-H**. We found that **2** has a half-life, $\tau_{1/2} = 49$ h in dry, degassed acetone at 295 K, which is almost 3 orders of magnitude longer than that for its constitutional isomer, **1-H**. Notably, aminyl radical **2** aggregates at ambient conditions in water and has a half-life, $\tau_{1/2} \approx 2$ h.

Results and discussion

The synthesis of aminyl radical **2** starts from commercially available carbazole, which is then converted to **3** in two steps according to the literature procedures (Scheme 1, SI).^{25,26} Then, **3** is converted to 1,8-di-*tert*-butyl-3,6-diiodo-9*H*-carbazole,²⁵ which is directly used in Pd-catalyzed cross-coupling with malonate,²⁷ to provide **4**. Alkylation of **4** with methyl iodide²⁷ gives **5**, which is then reduced with LiAlH₄ to yield tetraol **6**. Subsequent Williamson etherification gave the carbazole **7**. Treatment of **7** with *n*-BuLi, followed by one-electron oxidation of the resultant *N*-centered anion using ferrocenium cation ($[\text{FeCp}_2][\text{BF}_4]$) at low temperature provided aminyl radical **2**. The blue solution of the radical was diluted with cold pentane and purified by column chromatography at -40 °C using deactivated silica gel.^{24,28} After removal of the solvents at -40 °C, **2** was characterized by paramagnetic ¹H NMR spectroscopy.^{29,30}

¹H NMR spectrum for dilute solution of **2** in acetone-*d*₆ shows only resonances corresponding to the protons with relatively low spin densities, i.e., those of mPEG₃ groups. Two very weak singlets in the aromatic region may be assigned to carbazole **7** (ca. 4% content) (Figure 2). EPR spin counting determinations indicated spin concentration of up to 95% for **2**. Thus, radical **2** can be obtained in much higher spin purity than **1**-H or **1**-D (32–63%).²⁴

Scheme 1. Synthesis of Aminyl Radical **2.**



EPR spectrum of 0.33 mM aminyl radical **2** in acetone show triplet of triplets patterns due to isotropic ¹⁴N hyperfine coupling of one *I* = 1 nitrogen with *A*(¹⁴N) = 19.2 MHz and ¹H hyperfine coupling of two *I* = 1/2 hydrogens with *A*(¹H) = 2.65 MHz.³¹ The *g*-value is near 2.003, as expected for an aminyl radical.³¹ UV-vis absorption spectrum for **2** in acetone has a moderately strong band at $\lambda_{\text{max}} = 668$ nm with $\varepsilon_{\text{max}} = (9.37 \pm 0.22) \times 10^3 \text{ L} \cdot \text{mol}^{-1} \cdot \text{cm}^{-1}$ (Figure 2).³³

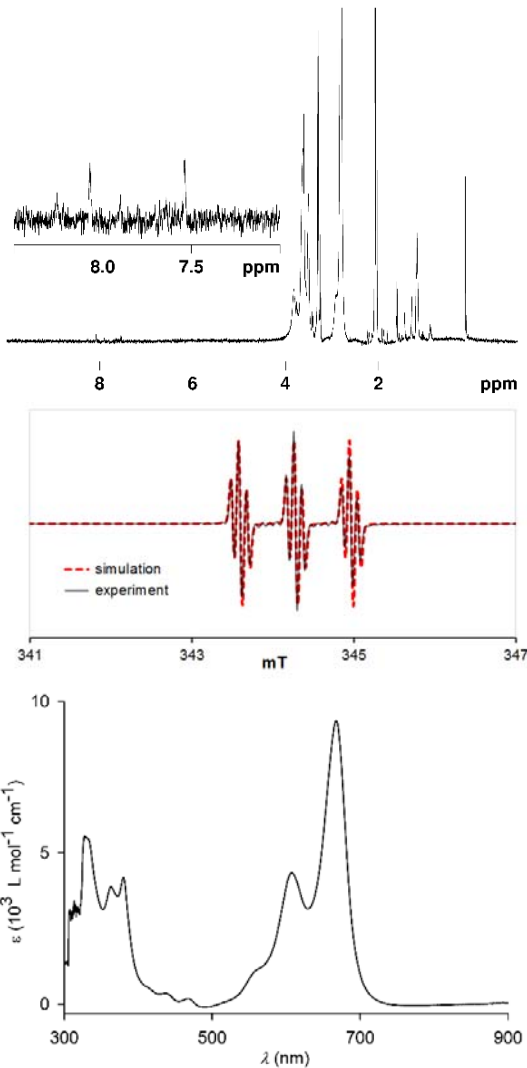


Figure 2. Top panel: Paramagnetic ^1H NMR (400 MHz) spectrum for 2.2 mM aminyl radical **2** in acetone- d_6 ; for this sample of **2**, both ^1H NMR spectra and EPR spectroscopic spin counting show spin concentration of about 95%. Residual acetone- d_5 and $\text{H}_2\text{O}/\text{HDO}$ peaks at $\delta \sim 2$ and ~ 3 ppm, respectively, are out of scale. Middle panel: EPR (X-Band, $\nu = 9.6519$ GHz) spectrum of 0.33 mM **2** in acetone, prior to the UV-vis absorption spectrum. Simulation: $g = 2.0031$, $A(^{14}\text{N}) = 19.2$ MHz ($n = 1$), $A(^1\text{H}) = 2.65$ MHz ($n = 2$), line-width = 0.05 mT, Lorentzian/Gaussian = 0.7. Bottom panel: The UV-vis absorption spectrum of **2** in acetone. More details may be found in the Experimental Section and the SI: Figures S1 – S7.

Aminyl radical **2** decays in degassed, dry acetone at the rate that is much slower than that of **1-H** or **1-D**. That is, **2** has a half-life $\tau_{1/2} = 49$ h at 295 K, compared to $\tau_{1/2} = 48$ sec for **1-H**,²⁴ and $\tau_{1/2} = 2.3$ h for **1-D**.

D.²⁴ This is expected because structure of **2** does not facilitate the intramolecular 1,5-HAT pathway with tunnelling. We note that both Arrhenius and Eyring plots for **1-H**, **1-D**, and **2** are linear and the slope in the Eyring plot of **2** corresponds to $\Delta H^\ddagger = 17.9$, kcal mol⁻¹, compared to those of **1-H** ($\Delta H^\ddagger = 10.0$),²⁴ and **1-D** ($\Delta H^\ddagger = 14.9$)²⁴ (Table 1 and Figure 3). Notably, the $\Delta H^\ddagger = 17.9$ kcal mol⁻¹ is still slightly below the nominal barrier of about 20 kcal mol⁻¹ computed for 1,5-HAT in **1-H**.²⁴

Table 1. Decay kinetics of **1-H**,²⁴ **1-D**,²⁴ and **2** in acetone: numerical fits to the Arrhenius and Eyring equations.^{a,b}

	T (K)	E_a (kcal/mol)	$\ln A$	ΔH^\ddagger (kcal/mol)	ΔS^\ddagger (e.u.)
1-H	182 – 298	10.5 ± 0.3	13.5 ± 0.8	10.0 ± 0.3	-33.3 ± 1.4
1-D	232 – 316	15.5 ± 0.8	17.1 ± 1.5	14.9 ± 0.8	-26.4 ± 2.9
2	274 – 316	18.5 ± 0.9	19.1 ± 1.5	17.9 ± 0.8	-22.6 ± 2.8

^a First order rate constants determined by either mid-field peak height of the EPR spectrum or paramagnetic susceptibility measured by SQUID (Fig. 3).

^b Error bars correspond to the 95% confidence intervals (Tables S1 – S3, SI).

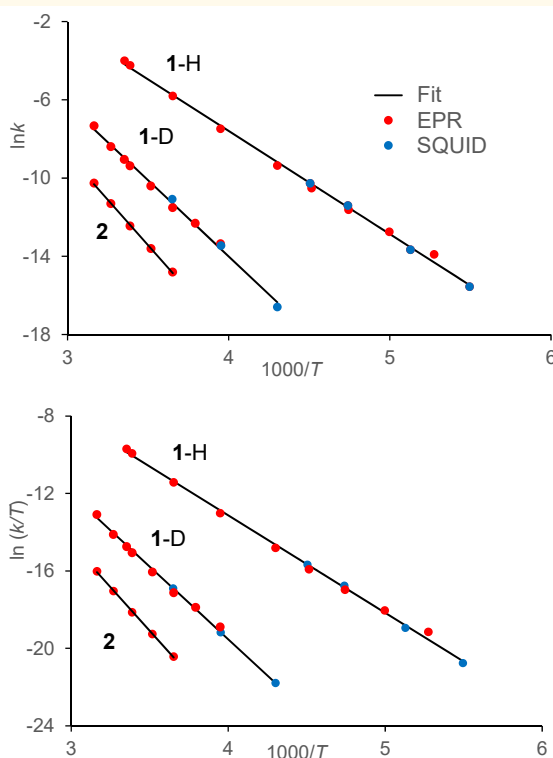


Figure 3. Decay kinetics of **1-H**, **1-D**, and **2** in degassed, anhydrous acetone. Numerical fits to the Arrhenius (top panel) and Eyring (bottom panel) equations are shown.

While the EPR spectra of **2** in acetone or DCM are sharp (Figure 2, Figs. S3 – S5, SI), the spectra of ~0.5 mM **2** in water are very broad (Figure 4), suggesting possible aggregation. As illustrated in Figure 5, the EPR spectrum in degassed water is broadened for **2** and relatively narrower for **1**-D.²⁴ Onset of aggregation is also evident in ¹H NMR spectroscopy of a more polar carbazole **7** in D₂O at 1 – 2 mM concentrations (Figs. S11 and S12, SI). However, the UV-vis absorption spectra of 0.05–0.5 mM **7** in water show a linear Lambert-Beer plot ($R^2 = 0.9999$), suggesting the absence of aggregation at these low concentrations (Fig. S9, SI). Notably, aminyl radical **2** in water decays at a much faster rate ($\tau_{1/2} \approx 2$ h at room temperature), compared to that of **2** in degassed acetone. When the decay of **2** in water is monitored by UV-vis spectroscopy, long-wavelength bands at $\lambda = 669, 610, 380$, and 364 nm, corresponding to **2**, are decreasing and short-wavelength bands at $\lambda = 242, 292, 322$, and 334 nm, corresponding to carbazole **7** (Fig. S8, SI), are increasing (Figure 4, middle panel). A weak long-wavelength increasing band at $\lambda \approx 430$ nm may correspond to trace amounts of carbazole nitroxide radical **2**-N (Scheme 2), derived from **2**. Several isosbestic points are observed.

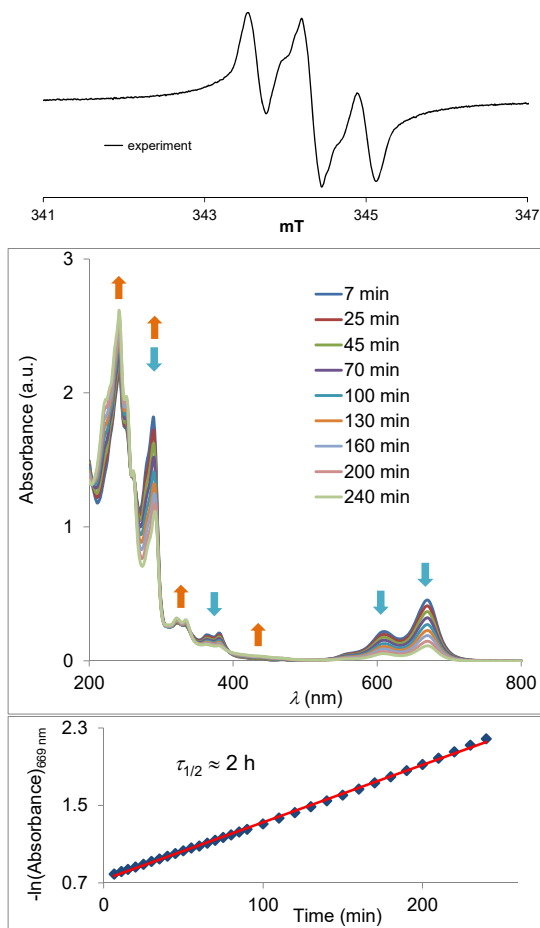


Figure 4. Top panel: EPR (X-Band, $\nu = 9.6519$ GHz) spectrum of 0.48 mM **2** in water, prior to the UV-vis absorption spectroscopic monitoring. Middle panel: UV-vis absorption spectroscopic monitoring of decay of aminyl radical **2** in water; initial spin concentration of **2** was 0.48 mM as measured by EPR spectroscopy. Isosbestic points are found at $\lambda = 526, 399, 340, 296$, and 260 nm. Bottom panel: negative $\ln(\text{Absorbance at } 669 \text{ nm})$ vs. time; half-life, $\tau_{1/2} = 116.9 \pm 1.4 \text{ min} (\pm 95\% \text{ CI})$.

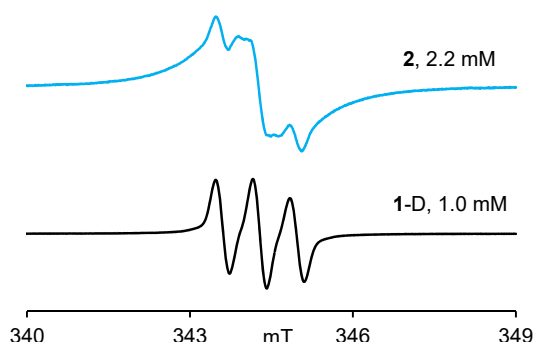
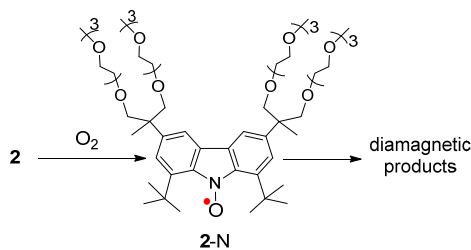


Figure 5. EPR spectra in degassed water for **2** and **1-D**.

We postulate that increased rate of decay of **2** in water may be associated with the aggregation bringing molecules of radical **2** (or carbazole **7**) in close proximity, and thus facilitating hydrogen transfer from OC-H moieties of mPEG-3 chains. Another possible explanation could be the presence of dissolved oxygen at ambient conditions in water, leading to the accelerated decay of **2** via carbazyl nitroxide radical **2-N** (Scheme 2).

Scheme 2. Decay of Aminyl Radical **2 in the Presence of Oxygen.**



To test the effect of dissolved O_2 , we carry out EPR experiments to monitor the decay of **2** in the following solvents: acetone saturated with O_2 , degassed water, and water saturated with O_2 . We observe that the decay of **2** is significantly accelerated in the solvent saturated with O_2 ; that is, the half-life of **2** decreases by one order of magnitude. In degassed water, **2** has $\tau_{1/2} = 6$ h, which is significantly longer than that in water at ambient conditions, $\tau_{1/2} \approx 2 - 3$ h, or in water saturated with O_2 , $\tau_{1/2} \approx 0.2$ h (Table S4, SI). For comparison, $\tau_{1/2} \approx 1$ h for **1-D** in degassed water is significantly shorter than that for **2**, presumably, because of significant contribution of 1,5-HAT in the decay of **1-D**.²⁴ We also detect a significant amount of nitroxide **2-N** in crude mixtures obtained from the decay of **2** in acetone saturated with O_2 and in water saturated with O_2 . Evidence for **2-N** is based on the EPR spectra^{28a,32,34} ($g = 2.0058$ vs 2.0033 for **2** and $A(^{14}N) = 21$ MHz vs 19 MHz for **2**) and by the detection of relatively intense (10–25% relative amplitude) ($M + Na$)⁺ ion for **2-N** (and related hydroxylamine) in the ESI MS (Figures S20 – S28 and S34 – S36, SI).

Finally, we determine that **2** has rather low 1H relaxivity, $r_1 = 0.025$ s^{-1} mM^{-1} at 7 Tesla, compared to $r_1 = 0.14$ s^{-1} mM^{-1} for the reference 3-carboxy-Proxyl nitroxide (Figure S38, SI).^{10a} This may provide

another evidence for aggregation of **2** in water that leads to poor access of water to hydrophobic radical centers.^{10a,11,23}

Experimental Section

General Procedures and Materials. For small scale reactions, tetrahydrofuran (THF) were vacuum transferred from sodium/benzophenone directly to the reaction vessel. All vacuum transfers were carried out using liquid nitrogen baths, unless indicated otherwise. *n*-BuLi (hexane) was obtained from commercial source; prior to use, the solution was diluted with hexane, which was dried over 12.5% (v/v) *n*-BuLi, and then it was added by vacuum transfer. The concentration of the resultant diluted solution was determined by titration with *N*-pivaloyl-*o*-toluidine.³⁵ All solvents were freshly distilled, e.g., toluene (from sodium), ether and THF (from sodium benzophenone), or alternatively obtained from solvent purification system. Per-deuterated solvents for NMR spectroscopy were obtained from commercial sources. All other chemicals were obtained from commercial sources, unless indicated otherwise.

Column chromatography was carried out on flash grade silica gel, using 0 – 20 psig pressure. Preparative TLC (PTLC) was carried out using tapered silica plates with a preadsorbent zone. Column chromatography and TLC for aminyl radical **2** was carried out on deactivated silica gel (typically, 3% triethylamine in pentane).²⁸ Standard techniques for synthesis under inert atmosphere, using Schlenk glassware and gloveboxes, were employed.

NMR spectra were obtained with commercial spectrometers (¹H, 400, 500, 600 or 700 MHz) using chloroform-*d* (CDCl₃), benzene-*d*₆ (C₆D₆), and acetone-*d*₆ as solvent. The chemical shift references were as follows: (¹H) chloroform-*d*, 7.26 ppm; (¹³C) chloroform-*d*, 77.16 ppm (chloroform-*d*), (¹H) benzene-*d*₅, 7.15 ppm; (¹H) acetone-*d*₅, 2.05 ppm; (¹³C) acetone-*d*₅, 29.84 ppm (acetone-*d*₆). Typical 1D FID was subjected to exponential multiplication with a line broadening exponent (LB) of 0.3 Hz (for ¹H) and 1.0 – 2.0 Hz (for ¹³C). For selected spectra, smaller (or negative) values of LB and additional Gaussian multiplication (GB) were used, to resolve closely spaced resonances, as indicated in the spectral data summaries. IR spectra were obtained using a commercial instrument, equipped with an ATR sampling accessory. UV-vis spectra were obtained on a commercial UV-vis-NIR spectrophotometer.

EPR Spectroscopy. CW X-band EPR spectra for aminyl radicals were acquired on a commercial instrument, equipped with a frequency counter and nitrogen flow temperature control (120–400 K). The spectra were obtained using a dual mode cavity, with an oscillating magnetic field perpendicular (TE₁₀₂) to the swept magnetic field; parallel mode (TE₀₁₂) was not used.

DPPH powder (*g* = 2.0037) was used as a *g*-value reference. Spin concentrations of aminyl radicals were measured in dichloromethane versus a 1.00 mM solution of a stable nitroxide radical (e.g., tempone) in dichloromethane at room temperature. Temperatures for kinetic studies were verified using an independently calibrated thin wire thermocouple inserted into the EPR sample tube (containing the solvent) and positioned in the cavity at the same place as in the kinetic studies. For kinetic studies, the samples were typically contained in 4-mm EPR sample tubes, equipped with high vacuum stopcocks; when acetone was used as a solvent, the tube was only partially inside the cavity of the instrument to maintain adequate Q-value or 0.8-mm O.D. thin-wall quartz capillaries were used. For EPR spectra in water, quartz capillaries were used.

Synthesis of 2. Chemicals and per-deuterated solvents for NMR spectroscopy were obtained from commercial sources and used as received unless otherwise indicated. Starting material, 1,8-di-*tert*-butyl-3,6-dinitro-9*H*-carbazole (**3**),^{25b} was prepared in two steps from carbazole, via 1,3,6,8-tetra-*tert*-butyl-9*H*-carbazole as intermediate, according to the literature methods.^{25,26}

Detailed summaries for preparation of all new compounds may be found in the SI.

Tetraethyl 2,2'-(1,8-di-*tert*-butyl-9*H*-carbazole-3,6-diyl)dimalonate (4). Compound **4** was obtained in 2-stage reaction, starting with conversion of starting material **3**^{25b} to 1,8-di-*tert*-butyl-3,6-diiodo-9*H*-carbazole, following literature procedure,^{25a} and then Pd-catalyzed double cross-coupling of malonate.²⁷

To **3** (2.06 g, 5.58 mmol) in THF (40 mL), Raney Ni suspension (6 mL) was added. After the reaction mixture was stirred under atmosphere of hydrogen gas (H₂-filled balloon) at 30 °C for overnight, TLC (silica, DCM/acetone, 7:3) analysis revealed disappearance of **3** and the clean formation of a new more polar product (diamine). The reaction mixture was filtered through celite, solvents were removed, and then the reaction flask was filled with nitrogen gas. Degassed 30% sulfuric acid (18 mL), and then

degassed aqueous solution (3 mL) of NaNO₂ (1.58 g, 22.9 mmol, 4 equiv) were added dropwise at 0 °C. After the reaction mixture was stirred for 30 min at 0 °C, then degassed aqueous solution (5 mL) of KI (6.0 g, 36.1 mmol, 6 equiv) was added dropwise. After stirring for overnight, the reaction mixture was subjected to aqueous work-up with ethyl acetate and brine. The organic layer was washed with aqueous Na₂S₂O₃ and brine, and then was concentrated and dried under vacuum. Column chromatography (silica gel, DCM/hexanes, 5:95) gave nearly pure 1,8-di-*tert*-butyl-3,6-diiodo-9*H*-carbazole (Figure S42),²⁵ which was used in the following reaction.

To 1,8-di-*tert*-butyl-3,6-diiodo-9*H*-carbazole (1.455 g, 2.74 mmol, 1.0 equiv) in a Schlenk vessel, K₃PO₄ (5.22 g, 24.6 mmol, 9.0 equiv) was added in a nitrogen filled glovebag. After the mixture was evacuated in Schlenk vessel for 18 h, then in a glovebag, Pd₂(dba)₃ (0.188 g, 0.205 mmol, 0.075 equiv) was added under N₂. After evacuation of the mixture for 3 h, then under the flow nitrogen gas, anhydrous toluene (6.0 mL), P(*t*-Bu)₃ (1.0 M solution in toluene, 1.1 mL, 1.1 mmol, 0.4 equiv), and diethyl malonate (distilled before use, 0.92 mL, 6.06 mmol, 2.2 equiv) were added.²⁷ The resultant suspension was stirred at ~70 °C for overnight, then was allowed to cool down to ambient temperature, quenched with saturated aqueous NH₄Cl solution and extracted with ethyl acetate. The organic layer was washed with brine, dried over sodium sulfate and concentrated in vacuum. The residue was purified on silica gel flash column chromatography (EA/hexanes, 10/90) to give the product **4** as a pale yellow solid (1.168 g, yield: 35% starting from **3** or 72% starting from 1,8-di-*tert*-butyl-3,6-diiodo-9*H*-carbazole). M.p.: 114–117 °C (under air). *R*_f 0.58 (EA/hexanes = 25/75). ¹H NMR (CDCl₃, 400 MHz): δ = 8.34 (s, 1H), 7.98 (d, 2H, *J* = 1.2 Hz), 7.36 (d, 2H, *J* = 1.6 Hz), 4.76 (s, 2H), 4.23 (m, 8H), 1.57 (s, 18H), 1.27 (t, 12H, *J* = 7.2 Hz). ¹³C NMR (CDCl₃, 100 MHz): aromatic region, expected 6 resonances; found 6 resonances at δ = 136.6, 132.6, 124.0, 123.9, 123.8, 119.1; aliphatic region, expected 6 resonances; found 6 resonances at δ = 168.7, 61.5, 58.1, 34.4, 30.2, 14.0. IR (ZnSe, cm⁻¹): 2963, 2904, 2869, 1731, 1600, 1576, 1501, 1465, 1396, 1386, 1367, 1302, 1275, 1215, 1142, 1095, 1031, 866, 764, 750. HRMS (ESI/TOF-Q) m/z (% RA for m/z): [M + Na]⁺ Calcd for C₃₄H₄₅NNaO₈ 618.3043 (100.0%), 619.3076 (36.8%); Found: 618.3055 (100%, 1.9 ppm), 619.3113 (18%, 6.0 ppm).

Tetraethyl 2,2'-(1,8-di-*tert*-butyl-9*H*-carbazole-3,6-diyl)bis(2-methylmalonate) (5). To the starting material **4** (1.168 g, 1.96 mmol, 1.0 equiv) and K₃PO₄ (Aldrich, 3.62 g, 17.1 mmol, 8.7 equiv), which were evacuated in a Schlenk vessel at ambient temperature for 1 day, then at 40 °C for another day, anhydrous toluene (5.0 mL) and iodomethane (0.75 mL, 12.0 mmol, 6.1 equiv) were added under a positive pressure of nitrogen gas.²⁷ The reaction mixture was stirred at 82–84 °C for 1 day. After cooling down to ambient temperature, the mixture was quenched with water, extracted with ethyl acetate, dried over sodium sulfate and concentrated in vacuum. The residue was purified on silica gel flash column chromatography (acetone/hexanes, 7.5/100) to give the product **5** as a pale yellow solid (0.61 g, yield: 50%). M.p. 151–154 °C (under air). *R*_f 0.42 (acetone/hexanes, 20/80). ¹H NMR (CDCl₃, 400 MHz): δ = 8.30 (s, 1H), 7.91 (d, 2H, *J* = 1.6 Hz), 7.38 (d, 2H, *J* = 1.6 Hz), 4.25 (m, 8H), 2.00 (s, 6H), 1.56 (s, 18H), 1.26 (t, 12H, *J* = 6.8 Hz). ¹³C NMR (CDCl₃, 100 MHz): aromatic region, expected 6 resonances; found 6 resonances at δ = 136.4, 131.9, 129.5, 123.7, 122.9, 116.8; aliphatic region, expected 7 resonances; found 7 resonances at δ = 172.4, 61.6, 59.0, 34.8, 30.5, 22.9, 14.2. IR (ZnSe, cm^{−1}): 2965, 2865, 1731, 1600, 1573, 1504, 1464, 1397, 1366, 1298, 1254, 1214, 1107, 1021, 924, 830, 736. HRMS (ESI/TOF-Q) m/z (% RA for m/z): [M + Na]⁺ Calcd for C₃₆H₄₉NNaO₈ at 646.3356 (100%), 647.3389 (40%); Found: 646.3353 (100%, −0.4 ppm), 647.3379 (32%, −1.5 ppm).

2,2'-(1,8-Di-*tert*-butyl-9*H*-carbazole-3,6-diyl)bis(2-methylpropane-1,3-diol) (6). After a suspension of lithium aluminum hydride (LiAlH₄, 16.0 mg, 0.42 mmol, 8.8 equiv) in anhydrous ethyl ether (0.3 mL) was stirred at 0 °C for 30 min, then to this mixture, a solution of compound **5** (29.9 mg, 0.048 mmol, 1.0 equiv) in anhydrous ethyl ether (0.6 mL) was added at 0 °C dropwise. The reaction mixture was stirred at 0 °C for another 30 min, then allowed to warm up to ambient temperature and stirred for overnight. Then, to the reaction mixture cooled with an ice bath, water was added slowly to quench the unreacted LiAlH₄, followed by extraction with ethyl acetate. The organic layer was dried over sodium sulfate and concentrated in vacuum. This crude mixture was combined with another one, obtained from 31.7 mg (0.51 mmol) of **5**, and purified on preparative thin-layer chromatography (DCM/acetone/EtOH, 60/40/3) to give the product **6** as a white solid (29.6 mg, yield: 65%). M.p. 288–291 °C (under argon atmosphere).

R_f 0.43 (DCM/acetone/EtOH, 60/40/3). ^1H NMR (acetone- d_6 , 700 MHz): δ = 8.26 (s, 1H), 8.09 (d, $J \approx 2$ Hz, 2H), 7.52 (d, $J \approx 2$ Hz, 2H), 3.99 (dd, $J_1 = 11$ Hz, $J_2 = 5$ Hz, 4H), 3.86 (dd, $J_1 = 11$ Hz, $J_2 = 5$ Hz, 4H), 3.60 (t, OH, 4H (readily exchanged in acetone- d_6), $J = 5$ Hz), 1.60 (s, 18H), 1.42 (s, 6H). ^{13}C NMR (acetone- d_6 , 100 MHz): δ = aromatic region, expected 6 resonances; found 6 resonances at δ = 136.6, 136.3, 132.6, 125.0, 122.2, 117.2; aliphatic region, expected 5 resonances; found 5 resonances at δ = 70.1, 45.6, 35.3, 30.7, 21.4. IR (ZnSe, cm^{-1}): 3344, 2963, 2923, 2872, 1494, 1466, 1423, 1395, 1381, 1366, 1297, 1263, 1235, 1089, 1032, 867. HRMS (ESI/TOF-Q) m/z (% RA for m/z): $[\text{M} + \text{Na}]^+$ Calcd for $\text{C}_{28}\text{H}_{41}\text{NNaO}_4$ at 478.2933 (100%), 479.2967 (30%); Found: 478.2927 (100%, -1.3 ppm), 479.2953 (22%, -2.9 ppm).

1,8-Di-*tert*-butyl-3,6-bis(7-methyl-2,5,9,12-tetraoxatridecan-7-yl)-9*H*-carbazole (7). To the finely ground dry KOH (0.45g, 8.02 mmol, 12.6 equiv) in a Schlenk vessel, the solution of starting material **6** (290.6 mg, 0.638 mmol, 1.0 equiv) in anhydrous THF (5 mL) and $\text{Ts}(\text{CH}_2\text{CH}_2\text{O})_3\text{Me}$ (1.60 mL, 4.96 mmol, 7.8 equiv) were added. The mixture was stirred at 65–66 °C for about 3 days. Then, the homogenous reaction mixture was diluted with water (20 mL) and extracted with ethyl acetate. The organic phase was dried over Na_2SO_4 then concentrated. The residue was purified 3 times with silica gel flash column chromatography (premium silica gel, DCM/acetone/EtOH, 80/20/2.4) to give the product **7** as light yellow oil (188.0 mg, yield: 28%). R_f 0.59 (DCM/acetone/EtOH, 75/25/3). ^1H NMR (acetone- d_6 , 400 MHz): δ = 8.26 (s, 1H), 8.07 (d, 2H, $J \approx 2$ Hz), 7.54 (d, 2H, $J \approx 2$ Hz), 3.77, 3.75 (AB, 8H, $J = 9$ Hz), 3.60 (s, 16H), 3.58–3.55 (m, 8H), 3.53–3.50 (m, 16H), 3.42–3.40 (m, 8H), 3.25 (s, 12H), 1.60 (s, 18H), 1.45 (s, 6H). ^{13}C NMR (acetone- d_6 , 100 MHz): δ = aromatic region, expected 6 resonances; found 6 resonances at δ = 136.9, 136.3, 132.3, 124.9, 122.4, 116.8; aliphatic region, expected 12 resonances; found 12 resonances at δ = 77.7, 72.6, 71.8, 71.3, 71.2, 71.1, 71.0, 58.8, 44.6, 35.4, 30.8, 22.3. IR (ZnSe, cm^{-1}): 2954, 2867, 1492, 1455, 1365, 1350, 1297, 1237, 1199, 1097, 1042, 851, 758. HRMS (ESI/TOF-Q) m/z (% RA for m/z): $[\text{M} + \text{Na}]^+$ Calcd for $\text{C}_{56}\text{H}_{97}\text{NNaO}_{16}$ at 1062.6705 (100%), 1063.6739 (60%), 1064.6772 (18.0%); Found: 1062.6681 (100%, -2.3 ppm), 1063.6759 (18%, -1.9 ppm), 1064.6764 (2%, -0.7 ppm).

UV-vis (water): $\lambda_{\text{max}}/\text{nm}$ ($\epsilon/\text{dm}^3 \text{ mol}^{-1} \text{ cm}^{-1}$) = 242 (2.2×10^4), 292 (7.2×10^3), 322 (2.1×10^3), 334 (1.9×10^3).

Aminyl radical 2. (This procedure uses $[\text{FeCp}_2][\text{BF}_4]$ as oxidant; an alternative procedure using iodine as oxidant is described in the SI.) To the Schlenk containing carbazole **7** (31.0 mg, 29.7 μmol , 1.0 equiv), which was dried under high vacuum at 64–69 °C for 2 days, anhydrous diethyl ether (0.15 mL) was added by vacuum transfer, to provide pale solution. After stirring the solution of **7** at –20 °C for 30 min, *n*-BuLi (0.3231 M in hexane, 135 μL , 43.6 μmol , 1.52 equiv) was added at –20 °C dropwise to give a yellow (with a pink tint) solution. The reaction mixture was stirred at –20 °C for 1 h, then stirred at ambient temperature for another hour. In this process, the color of the reaction mixture turned into light orange. Then, at –40 °C, ferrocenium tetrafluoroborate (8.4 mg, 30.8 μmol , 1.03 equiv, dried under high vacuum at rt for overnight before use) was added as a solid under the flow of argon gas. A deep blue color formed immediately, then turned into dark blue within minutes. The mixture was stirred at –40 °C for 3 h, then the solvents were removed high vacuum at –40 °C. Subsequently, the Schlenk vessel was charged back with argon gas, and then cold acetone (–78 °C, 0.2 mL, dried over CaSO_4 then distilled before use) was added, and subsequently evaporated under high vacuum at –40 °C, to remove the possible remnants of THF. The resultant dark blue solid was stored at –78 °C before purification (Figure S1, SI). The crude mixture of **2** was purified by silica gel flash column chromatography (silica gel deactivated with 3% Et_3N , acetone/hexanes (5/95 v/v) then acetone/hexanes (40/60 v/v) as the eluent) at –40 °C in a glove bag under nitrogen atmosphere.^{24,28} The received blue solution was transferred to a Schlenk vessel at –40 °C in a glove bag, then the Schlenk vessel was attached to high vacuum line. The solution of **2** was concentrated under high vacuum at –40 °C to give **2** (EPR spin conc. 95%) as a pasty at –40 °C, which solidified at –78 °C. For paramagnetic ¹H NMR spectrum of this sample of **2**, see: Figure S2, SI. UV-vis (acetone): $\lambda_{\text{max}}/\text{nm}$ [$\epsilon_{\text{max}}/\text{L mol}^{-1} \text{ cm}^{-1}$] = 607 [$(4.28 \pm 0.08) \times 10^3$], 668 [$(9.4 \pm 0.2) \times 10^3$ (mean \pm 95% CI)]. In another run starting from 31.0 mg (29.8 μmol) of **7**, 30.6 mg (99%) of **2** with spin concentration of about 90% was obtained.

Kinetic Studies. Samples for kinetic studies of decay of **2** in dry and degassed acetone were prepared as described before for **1-H** and **1-D**.²⁴

Sample for kinetic studies of decay of **2** in acetone saturated with O₂ (acetone/O₂) was prepared by adding acetone/O₂ (0.55 mL) to **2** (0.62 mg) in a vial flashed with O₂. Subsequently, part of the solution (0.15 mL) was transferred to a Schlenk 4-mm EPR tube (filled with O₂) under the flow of O₂ gas. The initial first order decay of **2** occurred with a half-life of 135 min (peak height monitoring) at 295 K (Figures S23–S25). After total of 43 hours at ambient temperature (Figure S26), light green reaction mixture was transferred to a vial and evaporated with N₂ gas. The resultant crude mixture was re-dissolved in degassed acetone, and then placed in a quartz capillary, to obtain EPR spectrum, showing aminyl radical **2** (69%) and nitroxide **2-N** (31%) (Figure S27). LR-MS (ESI) of the crude mixture showed a peak at *m/z* 1077.8 (relative amplitude of 20–25%) corresponding to [M+Na]⁺ ion for **2-N** (Figures S21 and S28).

Sample for kinetic studies of decay of **2** in degassed water was prepared by transferring degassed water (flashed with argon gas for 30 min) to aminyl radical **2** to provide a solution with 3.1 – 4.4 mM spin concentration. Subsequently, some of the solution was placed in a quartz capillary (sealed with parafilm) and then placed in 4-mm EPR tube (sealed with parafilm). EPR spectral monitoring gave half-life, $\tau_{1/2} \approx 6$ h (both by peak-height and double integration) at 295 K (Figures S29 and S30).

Sample for kinetic studies of decay of **2** in water saturated with O₂ (water/O₂) was prepared by adding water/O₂ (1.7 mL) to **2** in a vial flashed with O₂, to give a solution with an initial spin concentration of 0.38 mM. The resultant blue solution was stirred at ambient temperature (298 K) under O₂ atmosphere (balloons filled with O₂). At selected time intervals, part of the solution was placed in a quartz capillary, and then placed in a blank 4-mm EPR tube for measurement of spin concentration; these measurements showed, $\tau_{1/2} \approx 0.2$ h (double integration) (Figure S34). After 58–60 min in water/O₂, a yellow solution, containing nitroxide **2-N** was obtained (Figure S35). The solution was transferred to a vial, evaporated with N₂ gas, and then dried under high vacuum. LR-MS (ESI) of the crude mixture showed a peak at *m/z* 1078.5 (relative amplitude of 10%) corresponding to [M+Na]⁺ ion for **2-N** (Figure S36).

Acknowledgements

We thank the National Science Foundation (CHE-1362454 and CHE-1665256) and National Institutes of Health (R01 EB-019950-01A1) for support of this research. We thank Professor Michael D. Boska (University of Nebraska Medical Center) for a measurement of relaxivity of **2**.

Supporting Information Available: additional experimental details and complete ref 31a. This material is available free of charge via the Internet at <http://pubs.acs.org>.

References

1. Berliner, L. J.; Jacob Grunwald, J.; Hankovszky, H. O.; Hideg, K. *Anal. Biochemistry* **1982**, *119*, 450–455.
2. (a) Schmidt, M. J.; Borbas, J.; Drescher, M.; Summerer, D. *J. Am. Chem. Soc.* **2014**, *136*, 1238–1241. (b) Wang, Y.; Paletta, J. T.; Berg, K.; Reinhart, E.; Rajca, S.; Rajca, A. *Org. Lett.* **2014**, *16*, 5298–5300.
3. Water soluble trityls: (a) Ardenkjær-Larsen, J. H.; Laursen, I.; Leunbach, I.; Ehnholm, G.; Wistrand, L. G.; Petersson, J. S.; Golman, K. *J. Magn. Reson.* **1998**, *133*, 1–12. (b) Reddy, T. J.; Iwama, T.; Halpern, H. J.; Rawal, V. H. *J. Org. Chem.* **2002**, *67*, 4635–4639. (c) Liu, W.; Nie, J.; Tan, X.; Liu, H.; Yu, N.; Han, G.; Zhu, Y.; Villamena, F. A.; Song, Y.; Zweier, J. L.; Liu, Y. *J. Org. Chem.* **2017**, *82*, 588–596.
4. Water soluble verdazyls: (a) Mayr, A. J.; Eastman, M. P.; Hartzell, C. J.; Dong, D.; McClellan, C. J. *Magn. Reson.* **1969**, *99*, 387–390. (b) Barclay, T. M.; Hicks, R. G.; Lemaire, M. T.; Thompson, L. K.; Xu, Z. Q. *Chem. Commun.* **2002**, 1688–1689. (c) Le, T.-N., Grewal, H., Changoco, V., Truong, V., Brook, D. J. R. *Tetrahedron* **2016**, *72*, 6368–6374.
5. Huang, S.; Paletta, J. T.; Elajaili, H.; Huber, K.; Pink, M.; Rajca, S.; Eaton, G. R.; Eaton, S. S.; Rajca, A. *J. Org. Chem.* **2017**, *82*, 1538–1544.

6. (a) Song, C.; Hu, K.-N.; Joo, C.-G.; Swager, T. M.; Griffin, R. G. *J. Am. Chem. Soc.* **2006**, *128*, 11385–11390. (b) Haze, O.; Corzilius, B.; Smith, A. A.; Griffin, R. G.; Swager, T. M. *J. Am. Chem. Soc.* **2012**, *134*, 14287–14290.

7. (a) Sauve'e, C.; Rosay, M.; Casano, G.; Aussénac, F.; Weber, R. T.; Ouari, O.; Tordo, P. *Angew. Chem., Int. Ed.* **2013**, *52*, 10858–10861. (b) Jagtap, A. P.; Geiger, M.-A.; Stoppeler, D.; Orwick-Rydmark, M.; Oschkinat, H.; Sigurdsson, S. T. *Chem. Commun.* **2016**, *52*, 7020–7023.

8. Hubbell, W. L.; Lopez, C. J.; Altenbach, C.; Yang, Z. *Curr. Opin. Struct. Biol.* **2013**, *23*, 725–733.

9. (a) Ni, Q. Z.; Daviso, E.; Can, T. V.; Markhasin, E.; Jawla, S. K.; Swager, T. M.; Temkin, R. J.; Herzfeld, J.; Griffin, R. G. *Acc. Chem. Res.* **2013**, *46*, 1933–1941. (b) Keshari, K. R.; Wilson, D. M. *Chem. Soc. Rev.* **2014**, *43*, 1627–1659.

10. (a) Rajca, A.; Wang, Y.; Boska, M.; Paletta, J. T.; Olankitwanit, A.; Swanson, M. A.; Mitchell, D. G.; Eaton, S. S.; Eaton, G. R.; Rajca, S. *J. Am. Chem. Soc.* **2012**, *134*, 15724–15727. (b) Sowers, M. A.; McCombs, J. R.; Wang, Y.; Paletta, J. T.; Morton, S. W.; Dreaden, E. C.; Boska, M. D.; Ottaviani, M. F.; Hammond, P. T.; Rajca, A.; Johnson, J. A. *Nature Commun.* **2014**, *5*, 5460. DOI: [10.1038/ncomms6460](https://doi.org/10.1038/ncomms6460).

11. Spagnol, G.; Shiraishi, K.; Rajca, S.; Rajca, A. *Chem. Comm.* **2005**, 5047–5049.

12. Neugebauer, F. A.; Fischer, H. *Angew. Chem., Int. Ed.* **1971**, *10*, 732–733.

13. Neugebauer, F. A.; Fisher, H.; Bamberger, H.; Smith, S. O. *Chem. Ber.* **1972**, *105*, 2694–2713.

14. Gallagher, N.; Olankitwanit, A.; Rajca, A. *J. Org. Chem.* **2015**, *80*, 1291–1298.

15. Rajca, A.; Olankitwanit, A.; Wang, Y.; Boratyński, P. J.; Pink, M.; Rajca, S. *J. Am. Chem. Soc.* **2013**, *135*, 18205–18215.

16. Rajca, A.; Wongsriratanakul, J.; Rajca, S. *Science* **2001**, *294*, 1503–1505.

17. (a) Rajca, A.; Wongsriratanakul, J.; Rajca, S. *J. Am. Chem. Soc.* **2004**, *126*, 6608–6626. (b) Rajca, A.; Wongsriratanakul, J.; Rajca, S.; Cerny, R. L. *Chem. Eur. J.* **2004**, *10*, 3144–3157. (c) Rajca, A.; Lu, K.; Rajca, S. *J. Am. Chem. Soc.* **1997**, *119*, 10335–10345. (d) Rajca, A.; Rajca, S.; Padmakumar, R. *Angew. Chem., Int. Ed. Engl.* **1994**, *33*, 2091–2093.

18. (a) Ratera, I.; Veciana, J. *Chem. Soc. Rev.* **2012**, *41*, 303–349. (b) Rajca, A. *Chem. Rev.* **1994**, *94*, 871–893

19. Luo, D.; Lee, S.; Zheng, B.; Sun, Z.; Zeng, W. D.; Huang, K. W.; Furukawa, K.; Kim, D.; Webster, R. D.; Wu, J. S. *Chem. Sci.* **2014**, *5*, 4944–4952.

20. Wingate, A. J.; Boudouris, B. W. *J. Polym. Sci., Part A: Polym. Chem.* **2016**, *54*, 1875–1894.

21. Curtiss, L. A.; Blander, M. *Chem. Rev.* **1988**, *88*, 827–841.

22. (a) Tóth, E.; Helm, L.; Merbach, A. E. *Top. Curr. Chem.* **2002**, *221*, 61–101. (b) Maliakal, A. J.; Turro, N. J.; Bosman, A. W.; Cornel, J.; Meijer, E. W. *J. Phys. Chem. A* **2003**, *107*, 8467–8475.

23. We thank one of the Reviewers for pointing out the importance of fast water exchange for high ^1H water relaxivity.

24. Wang, Y.; Olankitwanit, A.; Rajca, S.; Rajca, A. *J. Am. Chem. Soc.* **2017**, *139*, 7144–7147.

25. (a) Neugebauer, F. A.; Fisher, H. *Chem. Ber.* **1972**, *105*, 2686–2693. (b) 1,8-di-*tert*-butyl-3,6-dinitro-9H-carbazole **3**: M.p.: 292–293 °C; lit.^{25a} M.p.: 289–290 °C. R_f = 0.29 (DCM/hexanes, 40/60); ^1H NMR (acetone- d_6 , 600 MHz): δ = 9.30 (d, 2H, J = 1.2 Hz), 8.39 (d, 2H, J = 1.2 Hz), 1.70 (s, 18H); ^1H NMR (CDCl₃, 400 MHz): δ = 8.96 (d, 3H, J = 2.0 Hz), 8.39 (d, 2H, J = 2.0 Hz), 1.66 (s, 18H); ^1H NMR (C₆D₆, 400 MHz): δ = 8.62 (d, 2H, J = 2.0 Hz), 8.42 (s, 1H, NH), 8.34 (d, 2H, J = 1.6 Hz), 1.12 (s, 18H).

26. (a) Moskalev, N. V. *Khimiya Gete rotsiklicheskikh Soedinenii* **1990**, *2*, 187–189. (b) Kuhn, N.; Schulten, M.; Boese, R.; Blaser, D. *Z. Naturforsch. B* **1991**, *46*, 1503–1508.

27. Beare, N. A.; Hartwig, J. F. *J. Org. Chem.* **2002**, *67*, 541–555.

28. (a) Rajca, A.; Takahashi, M.; Pink, M.; Spagnol, G.; Rajca, S. *J. Am. Chem. Soc.* **2007**, *129*, 10159–10170. (b) Vale, M.; Pink, M.; Rajca, S.; Rajca, A. *J. Org. Chem.* **2008**, *73*, 27–35.

29. la Mar, G. N., Ed., *Nuclear Magnetic Resonance of Paramagnetic Macromolecules*, 1995, Springer, Netherlands, pp. 1 – 391.

30. (a) Olankitwanit, A.; Kathirvelu, V.; Rajca, S.; Eaton, G. R.; Eaton, S. S.; Rajca, A. *Chem. Commun.* **2011**, *47*, 6443–6445. (b) Gallagher, N. M.; Bauer, J. J.; Pink, M.; Rajca, S.; Rajca, A. *J. Am. Chem. Soc.* **2016**, *138*, 9377–9380.

31. (a) Frisch, M. J. *et al.* *Gaussian 09*, Revision E.01, Gaussian, Inc., Wallingford CT, **2009**.
(b) UB3LYP/6-31G(d,p)-computed isotropic hyperfine coupling constants for TTBC: $A(^{14}\text{N}) = +22.47$ MHz, $A(^1\text{H}) = +4.15$ MHz (2H) and $A(^1\text{H}) = +0.77$ MHz (2H) (Table S5, SI). Assuming that the ratio of 5.3 between the computed values of $A(^1\text{H})$ for the two types of *meta*-protons is similar to the ratio between the experimental values of $A(^1\text{H})$ (ref 30), then the predicted experimental value for the smaller $A(^1\text{H}) \approx 0.5$ MHz for *meta*-protons would be well within the linewidth of 0.05 mT (~ 1.4 MHz) of the spectrum.

32. Olankitwanit, A.; Pink, M.; Rajca, S.; Rajca, A. *J. Am. Chem. Soc.* **2014**, *136*, 14277–14288.

33. Similar UV-vis absorption pattern was reported for a transient aminyl radical derived from carbazole: DiLabio, G.; Litwinienko, G.; Lin, S.; Pratt, D. A.; Ingold, K. U. *J. Phys. Chem. A* **2002**, *106*, 11719–11725.

34. Gerson, F.; Huber, W. *Electron Spin Resonance Spectroscopy of Organic Radicals* . Wiley-VCH: Weinheim, 2003, pp. 290 – 301.

35. Suffert, J. *J. Org. Chem.* **1989**, *54*, 509–510.